Scientific Papers of
the Department of Electrical Power Engineering of
the Wrocław University of Science and Technology

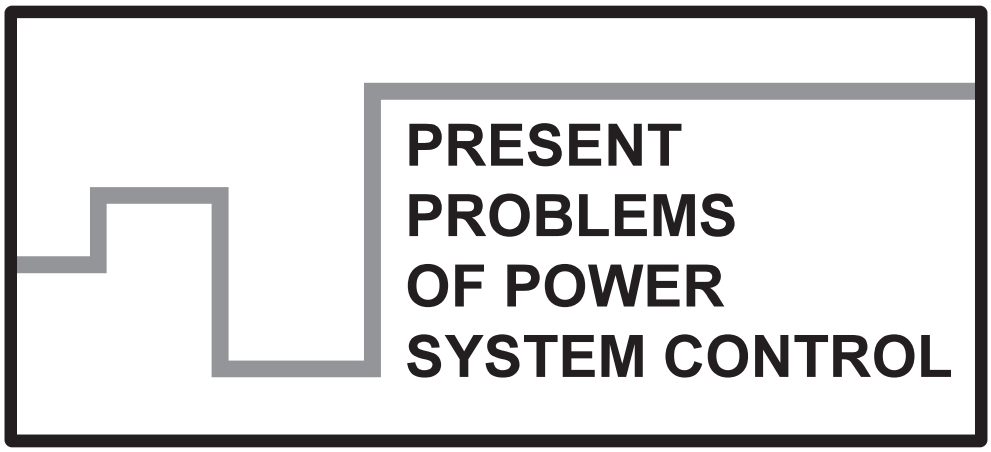

9

Wrocław 2018

Printed in the camera ready form

Department of Electrical Power Engineering
Wrocław University of Science and Technology
Wybrzeże Wyspiańskiego 27, 50-370 Wrocław, Poland
phone: +48 71 320 35 41
www: http://www.weny.pwr.edu.pl/instytuty,52.dhtml; http://www.psc.pwr.edu.pl
e-mail: wydz.elektryczny@pwr.edu.pl

OFICYNA WYDAWNICZA POLITECHNIKI WROCŁAWSKIEJ
Wybrzeże Wyspiańskiego 27, 50-370 Wrocław
http://www.oficyna.pwr.edu.pl
e-mail: oficwyd@pwr.edu.pl
zamawianie.ksiazek@pwr.edu.pl

ISSN 2084-2201

Print and binding: beta-druk, www.betadruk.pl

CONTENTS

Present Problems of Power System Control. 9, 2018

micro resistance welding, supercapacitor,
capacitive energy storage, flyback converter

Yuliia KOZHUSHKO*, Tetiana KARBIVSKA*,
Denys ZINCHENKO*, **, Danijel PAVKOVIĆ***,
Eugeniusz ROSOLOWSKI****, Oleksandr BONDARENKO*

CHARGING DEVICE OF CAPACITIVE ENERGY STORAGE FOR MICRO RESISTANCE WELDING

Micro resistance welding is the most common technology for making permanent connection between two conducting materials. This paper proposes a high-efficiency charging device for the capacitive energy storage within the micro resistance welding device power supply utilizing a Flyback converter. Based on the comprehensive analysis of charging device losses, it is determined that one of the main sources of conduction losses in the charging device is the output diode. In order to ameliorate this problem, utilization of a MOSFET transistor as an output diode within the Flyback converter is proposed in order to increase its overall efficiency. The presented results suggest that the proposed Flyback converter topology could improve the power efficiency by 7.0% at 50 kHz switching frequency through minimization of conduction losses in comparison with the traditionally-used Schottky diode.

1. INTRODUCTION

Micro resistance welding is one of the most effective welding technologies widely used by the electronics industry today. Micro resistance welding is performed between two pieces of conducting material by means of resistive heating caused by the passage of high-magnitude electric current [1].

The current amplitude for micro resistance welding typically ranges from hundreds to thousands of amperes and depends on material type and thicknesses of individual parts. Energy consumption of significant power and short duration followed by long pauses between each pulsed welding discharge are load features of the micro resistance welding device. These features determine the negative impact of welding equipment on

* National Technical University of Ukraine "Igor Sikorsky Kyiv Polytechnic Institute", Kyiv, Ukraine.
** Tallinn University of Technology, Tallinn, Estonia.
*** University of Zagreb, Zagreb, Croatia.
**** Wrocław University of Science and Technology, Wrocław, Poland

the utility electrical grid in terms of high-magnitude pulsed loads and voltage drops at the point of grid connection, and possible harmonic distortion of the grid voltage if switched AC power supply is used. One of the effective methods for mitigating of this problem is using suitable Energy Storage topology within the power supply for the welding equipment. The operation of such power supplies can be based on the capacitive energy storage, which can provide fast energy discharge required for the welding process during the required time interval [2]. Moreover, during charging of the capacitive energy storage, energy is consumed from the grid evenly, almost without a negative influence on it. Capacitive energy storage of the power supply has to accumulate enough energy to provide hundreds of thousands of charge/discharge cycles and ensure fast and efficient energy transfer to the load [2].

Due to the high energy density, Li-ion battery is commonly applied as energy storage in mobile devices. However, the high-amplitude pulsed load, which is inherent to the welding equipment, drastically degrades the operational characteristics and the useful cycle life and calendar life of the Li-ion battery [3]. An effective solution for micro resistance welding power supply is using supercapacitors. Due to high capacity, low leakage current, thermal characteristics, shelf life, supercapacitors could be used as capacitive energy storage of power supply for micro resistance welding [4].

Charging devices for capacitive energy storage have to provide significant current and low terminal voltage, because of peculiarities of the load. Moreover, energy efficiency and parameters of weight and size are the key parameters in the design of charging devices. Small size and weight could be achieved due to the increase in the switching frequency. However, the increase of the switching frequency causes a rise in the dynamic power losses. Conduction losses of the low-power converter are dependent on the current passing through the semiconductor components and they significantly reduce efficiency. Thus, choice of the optimal converter topology and thorough losses analysis are key points for the design of high-efficiency charging device [5].

Designing supercapacitor charging devices is an specific problem, which is discussed by a number of authors. For example, [5], [6] propose a supercapacitor charging device using a soft-switching full-bridge pulse-width modulated (PWM) converter. The proposed converter has the advantages of lower switch voltage stresses and reduced circulating current. A buck dc-dc converter is presented in reference [7] and used for supercapacitor charging. This paper describes the converter circuit by using a system of differential equations, and shows that the converter is capable of stable operation subject to different distortion sources. Reference [8] presents the converter for supercapacitor charging, that uses a resonant inverter, which can start its operation directly in steady mode, hereof can work in a mode close to short-circuit at the load side. It should be noted, however, that the authors of these papers do not consider the peculiarities of the load characteristic of the micro resistance welding process.

Thus, the aim of the work is to improve the circuit topology of the charging device for the capacitive energy storage of power supply for micro resistance welding.

2. CHARGING DEVICE FOR THE CAPACITIVE ENERGY STORAGE OF POWER SUPPLY FOR MICRO RESISTANCE WELDING

The developed circuit topology of the power supply for welding Multicell Pulse Generator is represented in Fig. 1.

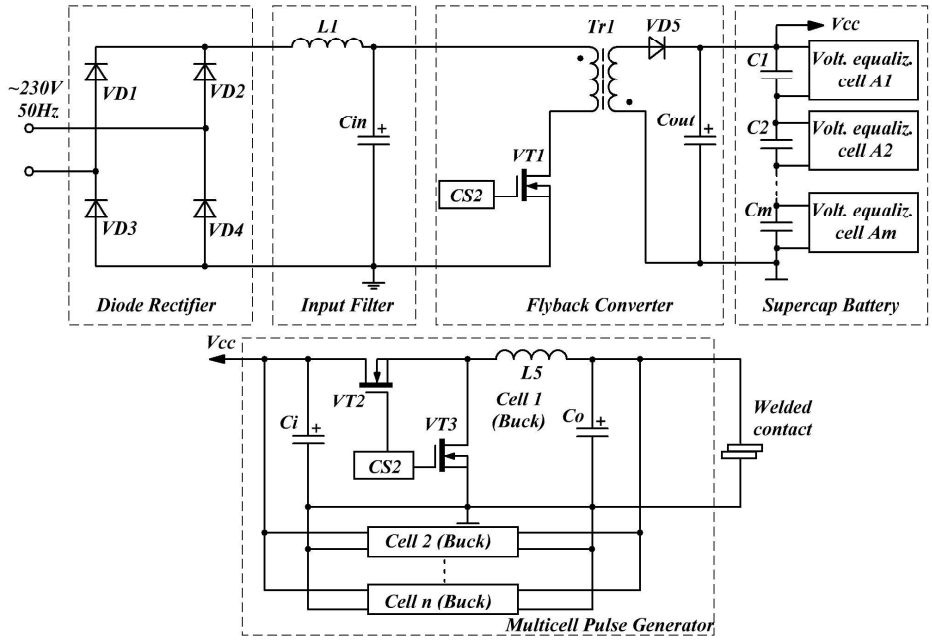

Fig. 1. Topology of power supply for micro resistance welding

This topology includes the following units. The Diode Rectifier rectifies the grid AC voltage with the frequency of 50 Hz, whereas the Input Filter smoothes the rectified (pulsed) DC voltage characterized by significant 100 Hz ripple. The Flyback Converter provides the voltage for charging the supercapacitor module. Multicell Pulse Generator regulates the welding current in the load. The Buck dc-dc converter topology is chosen as the basis for converter cells control under welding conditions.

The power supply is, in fact, a charger for the energy storage – the Supercap Battery, which includes *m* supercapacitors (350 F each) connected in series

The load of the circuit is the Supercap Battery. In this specific case, the main criteria for the choice of supercapacitor type are not a capacitance but an equivalent series resistance (ESR), which should be as small as possible. The analysis showed that the decrease of supercapacitor ESR is typically accompanied by the increase of its capacitance, and vice versa. The energy efficiency of the supercapacitor battery during discharge is defined by the following equation [9]:

$$\eta_c = \frac{W_U - W_{loss}}{W_U}, \tag{1}$$

where W_{loss} is the energy dissipated on the supercapacitor equivalent series resistors, and W_U is the usable energy within the supercapacitor, given by:

$$W_U = \frac{1}{2}CU_{\max}^2 - \frac{1}{2}CU_{\min}^2, \tag{2}$$

where $U_{\max}$ denotes the rated supercapacitor voltage and $U_{\min}$ represents the minimum allowed supercapacitor voltage once the discharge is finished.

Figure 2 shows the efficiency dependence on the discharging current for the supercapacitor cells whose parameters are listed in Table 1. Energy losses on the equivalent series resistors during the discharge of the supercapacitor are given by:

$$W_{loss} = R_{ESR} i_{disch}^2 t_{disch}, \tag{3}$$

where i_{disch} is the discharge current of the supercapacitor battery, R_{ESR} is the equivalent series resistance and t_{disch} is the discharging time.

Table 1. Parameters of supercapacitor cells from different manufacturers

Manufacturer	Rated voltage	Rated capacitance	Maximum ESR
Maxwell	2.7 V	350 F	3.2 mΩ
Nesscap	2.7 V	360 F	2.9 mΩ
Samwha	2.7 V	360 F	3.8 mΩ

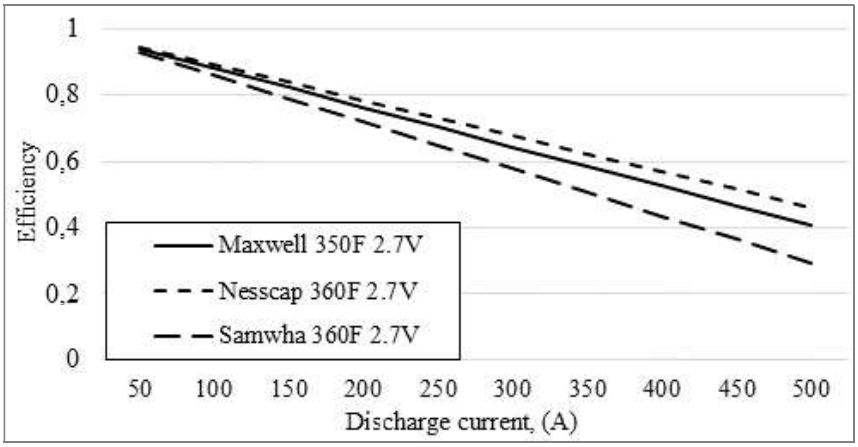

Fig. 2. Efficiency *vs*. discharging current bar graphs for different supercapacitor batteries

So, the choice of supercapacitor type with appropriate ESR ensures the required energy capacity for micro resistance welding, which does not need overly excessive, as in other applications, such as electric vehicles [10] and intermittent wind energy systems [11].

The converter, which controls the charging process of the supercapacitor battery, is designed as a Flyback converter. It partly functions as input current form corrector. It should be noticed that even though the output power of the converter is relatively low (tens of watts), the currents flowing through the considered part of the converter are several amperes and they cause substantial energy losses within individual circuit components. So, this part of the circuit requires an in-depth analysis.

3. ANALYSIS OF LOSSES OF THE CHARGINGING DEVICE

Energy efficiency is one of the key parameters in the design of charging devices. The efficiency of the charging device depends on the operating conditions such as the average value of voltage and current, and the PWM switching frequency. However, the most significant portion of total losses of the charging device is related to dynamic losses in semiconductors and conduction losses that are caused by parasitic resistances. Efficiency is usually expressed as [12]:

$$\eta = \frac{P_{out}}{P_{in}} \cdot 100\%, \tag{4}$$

where $P_{out} = P_{in} - P_{loss}$ is the device output power of the charging device, and P_{in} is the input power of the charging device.

As illustrated in Fig. 1, the charging device consists of a bridge rectifier, an input filter, a flyback converter, and a supercapacitor battery. Therefore, according to the proposed method, the total power losses are calculated as the sum of the power losses of each of the aforementioned subsystem of the charging device.

Power losses in the power supply of the charging device (i.e., input rectifier) are mainly caused by the conduction losses within the diodes due to the forward and reverse current flows. Switching (commutation) losses are negligible due to the low frequency of the alternating current supplying the charging device from the utility grid. The voltage drop across the diode and the series resistance are the sources of a diode's conduction losses [12], [13]:

$$P_{VDcond} = I_d^2 \cdot R_{DS} + I_{in} \cdot U_F, \tag{5}$$

where I_d is the RMS value of the current passing through diode, R_{DS} is the equivalent resistance of the diode, U_F is the forward voltage drop and I_{out} is the input current of the charging device (bridge rectified output current).

During conduction, the power loss in each of the two simultaneously conducting diodes will be the same. Since only a pair of diodes are conducting over one half-period of the grid voltage, the average power loss within the diode bridge rectifier can be calculated as:

$$P_{rectifier} = \frac{2}{T}\int_0^{T/2} 2P_{VDcond}dt = 2P_{VDcond}\,. \tag{6}$$

Power losses within the input filter generally comprise the inductor and capacitor power losses. Dielectric power losses of the input capacitor C_{in} can be calculated from the following equation [12]:

$$P_C = U_C \cdot 2\pi fC \cdot \tan\delta\,, \tag{7}$$

where U_c is the capacitor voltage, C is the capacitor capacitance, and $\tan\delta$ is the dielectric loss angle tangent.

Inductor losses are due to the core hysteresis losses and winding losses, while the eddy current losses are neglected due to the frequency of the voltage at the filter input. In order to calculate the losses in the inductor core, the following equation can be used [14]:

$$P_{Lc} = k \cdot f^{\alpha} \cdot B^{\beta} \cdot V_c\,, \tag{8}$$

where f is the rectified voltage ripple frequency (twice the grid voltage frequency), B is the magnitude of flux density variations within the core, and k, α and β are Steinmetz's constants and V_c is the volume of core material.

The wire (conductor) loss, caused by the Ohmic resistance, is defined by the following formula:

$$P_{Lw} = I_d^2 \cdot R_{DC}\,, \tag{9}$$

where I_d is the RMS value of the current passing through inductor, and R_{DC} is the winding Ohmic resistance.

Power losses of the Flyback converter consist of the transformer losses, MOSFET transistor losses, output Schottky diode losses, and output capacitor losses. Transformer power losses can be categorized as: core hysteresis losses, core eddy current losses, and winding losses.

The hysteresis losses represent the work required in order to alternate the direction of the magnetic flux within the ferromagnetic core. Naturally, these losses strongly depend on the type of material used to build the core. Based on the improved Steinmetz equation, the transformer core power losses P_{Trc} can also be calculated according to Eq. (6), wherein the parameter B represents the magnitude of the alternating magnetic field flux density within the core [14]:

$$P_{Trc} = k \cdot f^{\alpha} \cdot B_m^{\beta} \cdot V_c\,. \tag{10}$$

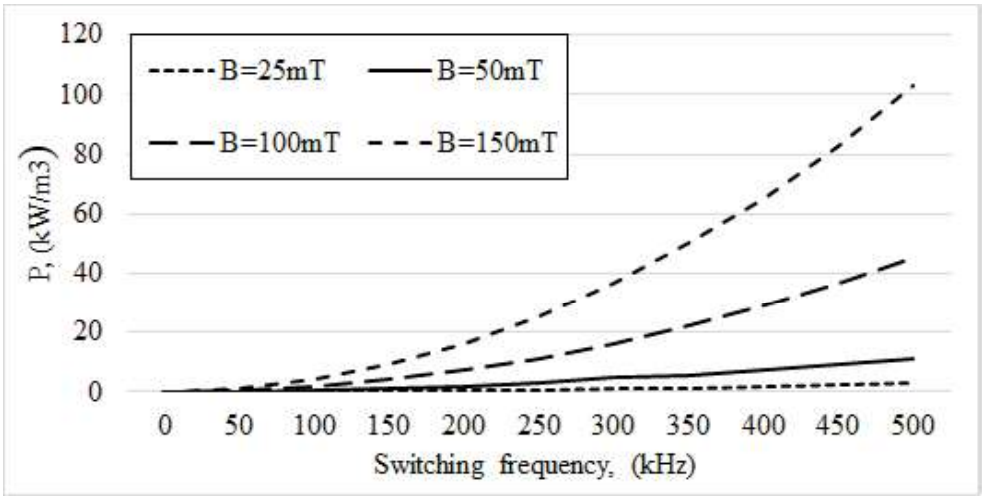

Fig. 3. Core hysteresis frequency power losses for different field flux density magnitudes

The transformer core hysteresis losses are proportional to the Flyback converter switching frequency and to the maximum amplitude (magnitude) of the magnetic field flux density. Figure 3 illustrates the core losses for a selected transformer as a function of field flux density magnitude and frequency. It is apparent that for very low magnitudes of the core field flux density (B = 50 mT), the core losses may be considered negligible up to 100 kHz. However, as the frequency and filed flux density increase, hysteresis losses may have a significant effect on the overall losses of the charging device.

The eddy currents generated by the magnetic field also contribute to the overall losses within the transformer core. The eddy currents flowing within the core will give rise to the so-called magnetic skin effect, which will also be more prominent at higher frequencies. As a consequence, the flux density in the core and the power flow through the transformer are reduced. Figure 4 shows the frequency dependence of the power losses due to eddy currents.

The power losses due to eddy currents are obtained according to the following equation [15]:

$$P_{Tre} = k_e \cdot f^2 \cdot B^2 \cdot V_c, \tag{11}$$

where f is the power converter PWM switching frequency, B is the flux density within the core, k_e is the eddy current coefficient that depends on the type of the core material and V_c is the volume of the core material.

The magnitude of the winding losses is proportional to the winding resistance, and to the current squared. The magnetic field around the windings will in turn create an electric skin effect, which will increase the effective resistance of the windings, thereby

restricting the current flow to the outer parts of the conductor. The winding power losses can be calculated as [12]:

$$P_{Trw} = \sum_{n=1}^{m} I_{DCn}^2 \cdot R_{DCn} + \sum_{n=1}^{m} I_{ACn}^2 \cdot R_{ACn}, \tag{12}$$

where I_{DC} is the DC current component, R_{DC} is the winding DC (Ohmic) resistance, I_{AC} is the AC current component, and R_{AC} is the winding equivalent AC resistance due to the electric skin effect.

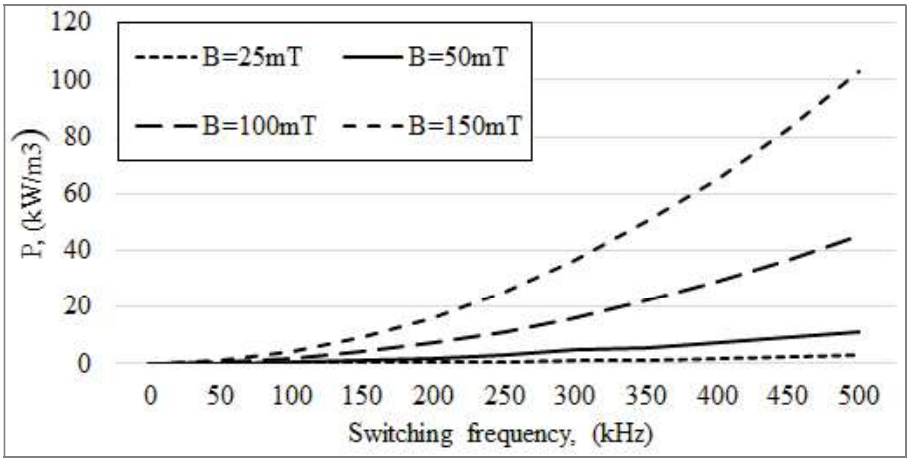

Fig. 4. Eddy current *vs*. frequency power losses for different magnitudes of field flux density

Conduction losses of the MOSFET transistor are directly dependent on the current passing through the transistor and are very little dependent on the switching frequency. Conduction losses within the power MOSFET can be calculated as [9]:

$$P_{VTcond} = I_d^2 \cdot R_{DS(on)}, \tag{13}$$

where I_d is the RMS value of the current passing through the transistor, and $R_{DC(on)}$ is the drain-source on-state resistance.

MOSFET switching losses depend on the load current and the power supply switching frequency according to the following equation [12]:

$$P_{VTsw} = U_{in} \cdot f \cdot (I_D \cdot t_a + 0{,}5 Q_{rr}), \tag{14}$$

where U_{in} is the drain-to-source voltage, I_D is the drain current, f is the switching frequency, t_a is the reverse recovery time, and Q_{rr} is the reverse recovery charge.

The conduction losses of the output Schottky diode within the Flyback converter are calculated as follows [11]:

$$P_{VDcond} = I_d^2 \cdot R_{DS} + I_{out} \cdot U_F \,, \tag{15}$$

where I_d is the RMS value of the current passing through diode, R_{DS} is the equivalent resistance at the given junction temperature of the diode, U_F is the forward voltage drop and I_{out} is the output current of the Flyback converter.
Finally, dielectric power losses of the output capacitor C_{out} can be calculated from (7).

The circuit schematic in Fig. 5 represents a simple RC model of a supercapacitor. It comprises three ideal circuit elements: a series resistor R_{ESR} (i.e. the equivalent series resistor or ESR) which contributes to the energy loss component of the supercapacitor during charging or discharging; a parallel resistor R_{leak} representing the leakage resistance, and a capacitor C_{SC} representing the supercapacitor capacitance. The power losses due to the leakage current are significantly lower than the power losses due to equivalent series resistance. Consequently, leakage current losses can be neglected in the analysis [9].

The power losses during charging of the supercapacitor can be calculated as:

$$P_c = i_c^2 \cdot \sum_{k=1}^{m} R_{ESRk} \,, \tag{13}$$

where i_c is the supercapacitor battery charging current and R_{ESR} is the equivalent series resistor of the k-th series-connected supercapacitor cell.

Supercapacitor charging current can be expressed by the following equation:

$$i_c = C_{SC} \frac{dU}{dt} \,, \tag{14}$$

where U is the voltage across the equivalent capacitor C_{SC}.

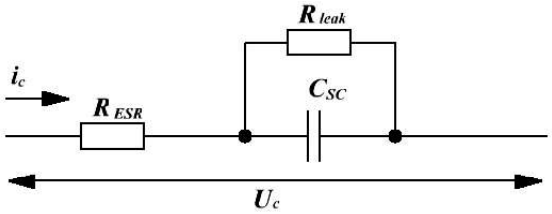

Fig. 5. Equivalent model of a supercapacitor

4. EFFICIENCY OF THE CHARGING DEVICE

Power losses have been evaluated analytically on the basis of the equations discussed in Sections 3. The main components data and parameters of the charging device are reported in Table 2.

Table 2. Data used in power losses analysis

U_{in}, V	230 ± 10%	*VD1–VD4*	KBP207G	*Tr1*	ferrite	N87
					core	EFD-25
U_{out}, V	5.5	C_{in}	4.7 µF, 400 V	*VD5*	STPS40L40CT	
I_{disch}, A	50–500	L_{in}	RLB0812-101KL	C_{out}	10 µF, 100 V	
f_{sw}, kHz	50–500	*VT1*	STB8N65M5	Supercap	Maxwell 350 F 2.5 V	

Based on the equations given in Sections 3, losses as a function of the converter switching frequency are presented in Fig. 6. One of the main sources of conduction losses in the charging device is the output diode VD5. The voltage drops in the open *p*-*n*-junction of the typical diode are 1.2–1.4 V. The problem could be solved application of Schottky diodes, in which the voltage drop is 0.4–0.7 V. Another way to solve the problem could be used a MOSFET transistor as an output diode of a Flyback converter [16].

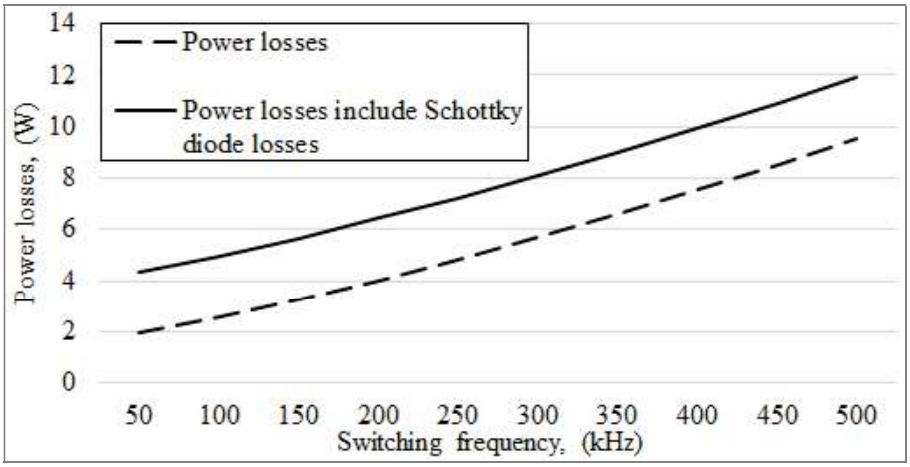

Fig. 6. Power loss as a function of the switching frequency

It should be mentioned that in order to determine the optimal topology of the charging device of Supercap Battery, it is necessary to carry out losses analysis for both topologies with the different values of the switching frequency, since the increase of the switching frequency dramatically increases the dynamic power losses. The function of switching frequency-related power losses in Fig. 7 shows the obtained results of power losses analysis for the Flyback converter topology based on using MOSFET transistor as an output diode.

Figure 8 shows the calculated efficiencies of the charging device for different values of switching frequency. The Flyback converter topology with Schottky diode as output diode achieves an efficiency of 85.0 % at 50 kHz switching frequency for a 28.6 W output power. On the other hand, the proposed converter with MOSFET transistor acting as

the output diode achieves a notably higher efficiency of 92.0 % at the same switching frequency and for equal output power conditions. Therefore, the proposed Flyback converter topology could improve the power efficiency by 7.0 % by minimizing the conduction losses.

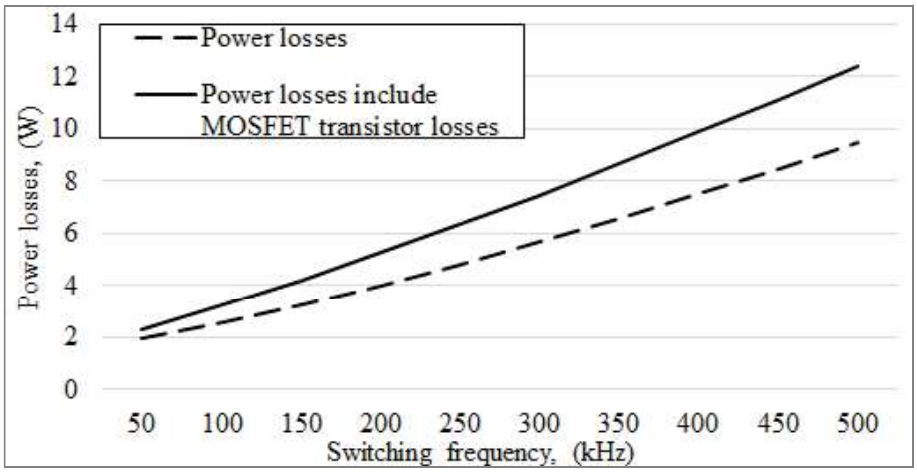

Fig. 7. Power loss as a function of the switching frequency

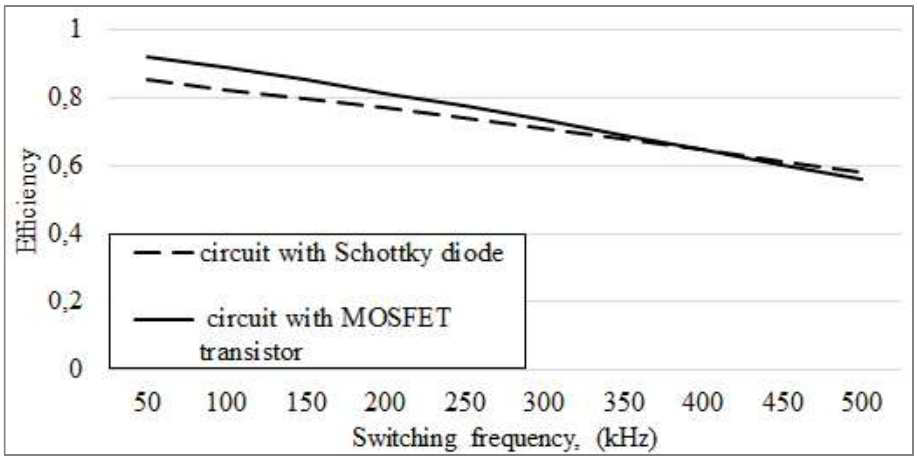

Fig. 8. Comparison of efficiency of the Flyback converter topology with Schottky diode and with MOSFET transistor

It should be noted that the increase in switching frequency increases the dynamic power losses of MOSFET transistor and thereby reduces the gain in efficiency. Fig.8 shows that using the MOSFET transistor as the output diode of the Flyback converter does not seem to be advisable at switching frequencies above 400 kHz.

5. CONCLUSIONS

This paper has presented an analysis of power losses within the Flyback converter used as a charging device for the supercapacitor-based energy storage system utilized in micro-resistance welding applications. The analysis results have pointed out to the possibility of notably increasing the efficiency of the charging device. The high-efficiency of the charging device could be provided by reducing the conduction power losses of the Flyback converter. The improved efficiency of the Flyback converter can be achieved by using a MOSFET transistor as an output diode, thus increasing the efficiency by 7.0% at the switching frequency of 50 kHz. However, the application of the MOSFET transistor is inadvisable at switching frequencies above 400 kHz, because the dynamic power losses of the MOSFET transistor increase above those observed for the case of the more traditionally used Schottky diode.

REFERENCES

[1] DONG S., KALKA G., ZHOU Y., *Electrode sticking during micro-resistance welding of thin metal sheets*, Electronics Packaging Manufacturing IEEE Transactions, 2002, Vol. 25, No. 4, 355–361, DOI: http://dx.doi.org/10.1109/ICEPT.2017.8046536.

[2] BONDARENKO Yu., SAFRONOV P., BONDARENKO O., SYDORETS V., ROGOZINA T., *The hybrid energy storages based on batteries and ultracapacitors for contact microwelding*, Tekhnologiya i konstruirovanie v elektronnoi apparature, 2014, No. 4, 33–38 (in Russian), DOI: http://dx.doi.org/10.15222/TKEA2014.4.33.

[3] SHEN J., DUSMEZ S., KHALIGH A., *Optimization of Sizing and Battery Cycle Life in Battery. Ultracapacitor Hybrid Energy Storage Systems for Electric Vehicle Applications*, IEEE Transactions on Industrial Informatics, 2014, Vol. 10, No. 4, pp. 2112–2121, DOI: http://dx.doi.org/10.1109/TII.2014.2334233.

[4] SHIN D., KIM Y., SEO J., *Battery-supercapacitor hybrid system for high-rate pulsed load applications*, Design, Automation & Test in Europe. Grenoble, France. March 2011, 627–632, DOI: https://doi.org/10.1109/DATE.2011.5763295.

[5] CHOI W., YANG M., SUH Y., *High-efficiency supercapacitor charger using an improved two-switch forward converter*, Journal of Power Electronics, 2014, Vol. 14, No. 1, 1–10, DOI: http://dx.doi.org/10.6113/JPE.2014.14.1.1.

[6] YANG M., CHO H., LEE S., CHOI W., *High-efficiency ultracapacitor charger using a soft-switching full-bridge DC-DC converter*, IEEE Applied Power Electronics Conference and Exposition (APEC). Charlotte, USA. March, 2015, 2044–2049, DOI: http://dx.doi.org/10.1109/APEC.2015.7104630.

[7] HRANOV T., VACHEVA G., HINOV N., ARNAUDOV D., *Modeling DC-DC converter for charging supercapacitors*. 40th International Spring Seminar on Electronics Technology (ISSE). Sofia, Bulgaria. May 2017, 1–5, DOI: http://dx.doi.org/10.1109/ISSE.2017.8001002.

[8] KRAEV G., HINOV N., ARNAUDOV D., RANGELOV N., GILEV B., *Serial ZVS DC-DC converter for supercapacitor charging*. 19th International Symposium on Electrical Apparatus and Technologies (SIELA), Bourgas, Bulgaria, May 2016, 193–196, DOI: http://dx.doi.org/10.1109/SIELA.2016.7543018.

[9] YANG H., ZHANG Y., *Analysis of supercapacitor energy loss for power management in environmentally powered wireless sensor nodes*, IEEE Transactions on Power Electronics, 2013, Vol. 28, No. 1, 5391–5403, DOI: http://dx.doi.org/10.1109/TPEL.2013.2238683.

[10] PAVKOVIĆ D., CIPEK M., KLJAIĆ Z., MLINARIĆ T.J., HRGETIĆ M., ZORC D., *Damping Optimum-Based Design of Control Strategy Suitable for Battery*, Ultracapacitor Electric Vehicles, Energies, 2018, Vol.11, No. 10, Paper No. 2854, 26 pp., DOI: https://doi.org/10.3390/en11102854.

[11] PAVKOVIĆ D., CIPEK M., HRGETIĆ, M, SEDIĆ A., *Modeling, parameterization and damping optimum-based control system design for an airborne wind energy ground station power plant*, Energy Conversion and Management, 2018, Vol. 164, pp. 262–276, DOI: https://doi.org/10.1016/j.enconman.2018.02.090.

[12] IVANOVIC Z., BLANUSA B., KNEZIC M., *Power Loss Model for Efficiency Improvement of Boost Converter*. XXIII International Symposium on Information, Communication and Automation Technologies. Sarajevo, Bosnia and Herzegovina, October 2011, 1–6, DOI: http://dx.doi.org/10.1109/ICAT.2011.6102129

[13] CAPITAINE A., PILLONNET G., CHAILLOUX T., KHALED F., ONDEL O., ALLARD B., *Loss analysis of flyback in discontinuous conduction mode for sub-mW harvesting systems*. 14th IEEE International New Circuits and Systems Conference (NEWCAS), Vancouver, Canada, June 2016, 1–4, DOI: http://dx.doi.org/10.1109/NEWCAS.2016.7604810.

[14] SULLIVAN C., HARRIS H., HERBERT E., *Core loss predictions for general PWM waveforms from a simplified set of measured data*. Proc. of Applied Power Electronics Conference and Exposition (APEC), Palm Springs, USA, February 2010, 1048–1055. DOI: http://dx.doi.org/10.1109/APEC.2010.5433375.

[15] FIORILLO F., BEATRICE C., BOTTAUSCIO O., CARMI E., *Eddy-Current Losses in Mn-Zn Ferrites*, IEEE Transactions on Magnetics, 2014, Vol. 50, No. 1, DOI: http://dx.doi.org/10.1109/TMAG.2013.2279878.

[16] SEMENOV B., *Power Electronics: from simple to complicated*, SOLON-Press, Moscow 2005, 416 (in Russian).